

Sharing the Load: Distributed Model-Predictive Control for Precise Multi-Rover Cargo Transport

Alexander Krawciw, Sven Lilge, Luka Antonyshyn, and Timothy D. Barfoot

Abstract—For autonomous cargo transportation, teams of mobile robots can provide more operational flexibility than a single large robot. In these scenarios, precision in both inter-vehicle distance and path tracking is key. With this motivation, we develop a distributed model-predictive controller (MPC) for multi-vehicle cargo operations that builds on the precise path-tracking of lidar teach and repeat. To carry cargo, a following vehicle must maintain a Euclidean distance offset from a lead vehicle regardless of the path curvature. Our approach uses a shared map to localize the robots relative to each other without GNSS or direct observations. We compare our approach to a centralized MPC and a baseline approach that directly measures the inter-vehicle distance. The distributed MPC shows equivalent nominal performance to the more complex centralized MPC. Using a direct measurement of the relative distance between the leader and follower shows improved tracking performance in close-range scenarios but struggles with long-range offsets. The operational flexibility provided by distributing the computation makes it well suited for real deployments. We evaluate four types of convoyed path trackers with over 10 km of driving in a coupled convoy. With convoys of two and three rovers, the proposed distributed MPC method works in real-time to allow map-based convoying to maintain maximum spacing within 20 cm of the target in various conditions.

I. INTRODUCTION

Transporting goods is one of the key applications for mobile robots. Warehouse robots have been deployed at massive scales, moving goods inside of controlled environments efficiently [1]. Outdoors, trucking promises to scale up the distance of autonomous cargo movement [2]. A significant body of autonomous driving research [3] works to enable safe operation of these massive vehicles. The largest autonomous vehicles are those used for construction [4] and resource extraction [5], [6], [7] payloads.

As delivery and logistics move off-road, there is interest in flexible systems that can be used for cargo transport in addition to other tasks. A system that is capable of using two independent vehicles to share a large piece of cargo provides more operational flexibility than a single, large vehicle. We use two smaller off-road robots with a cargo that is too bulky for one vehicle. Fig. 1 shows our experimental platform transporting a 23 kg Pelican case.

Teach and repeat [8] has proven to be a reliable method for ground-vehicle navigation in unstructured, GNSS-denied environments. Teach and repeat works by creating a topometric map of an environment while the robot is driven manually. This topometric map defines the valid set of routes to repeat along and stores metric map representations for

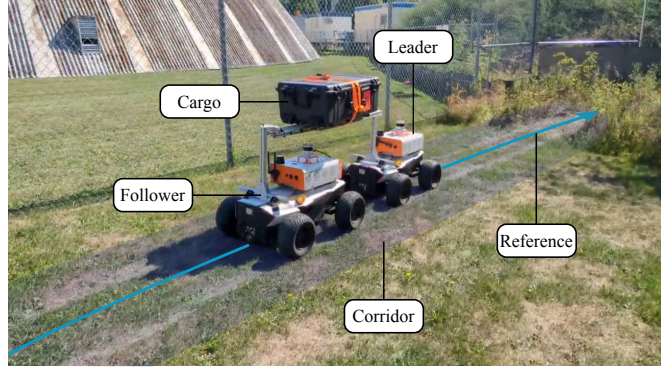


Fig. 1. A coupled robot convoy navigating the Woody Loop while cooperatively carrying cargo. A common set of tracks is clearly visible showing the two robots following each other within a few centimetres of error laterally and longitudinally.

localization. Teach and repeat was first implemented using cameras [8], but implementations exist that use radar [9], and lidar [10]. In this work, lidar teach and repeat is selected for its high accuracy and illumination invariance. Teach and repeat is well-suited to off-road cargo transport as shipments will require multiple traversals between a small set of known places.

This paper extends teach and repeat into a multi-robot convoying system. Using a single teach, a convoy of robots can repeat in unison. A distributed model-predictive controller (MPC) is developed that allows a heterogeneous fleet of vehicles to convoy together. Depending on the operational requirements of the repeat, the vehicles can convoy coupled by a piece of cargo carried between them. We compare four controllers for coordinated cargo transport over terrains with various roughness and slopes.

Section II describes related work focused on coupled cargo transport vehicles as well as a brief look at other approaches to coordinated motion. Section III describes the kinematic model used for this work and the formulation of the MPC. Section IV describes our experimental platforms and testing routes. Section V compares the performance of two-robot convoys with four different controllers. Section VI evaluates observations of the proposed system and demonstrates its scalability to larger convoys and adaptability to different objectives. Finally, Section VII concludes by reiterating the relative strengths of each MPC approach and evaluating the situations in which each is best suited.

II. RELATED WORK

A convoy refers to a group of vehicles or robots that move in a coordinated manner [11]. There has been a significant

amount of interest in convoying for both trucking (where they are also called platoons [12]) and military vehicles [11].

Zhao et al. [13] present a convoy of two or three Jeep-style vehicles that drive on gravel roads at approximately 30 km/h with maximum inter-robot distance errors of less than 10 m. They use a combination of shared GNSS positions fused with camera and lidar tracking of the leader. Their approach includes the ability of the follower to deviate from the leader's path to avoid encroaching obstacles. Vasseur et al. [14] also follow using cameras to measure the preceding vehicles' position. However for long inter-vehicle distances, the lead vehicle will not be detectable by its followers. In this case, the leader sends data about its motion to the followers and let them use a common localization to follow. In essence, this is a version of multi-robot teach and repeat. For large separations, path tracking is the only objective. Bienemann et al. [15] develop a convoy using two cars driving on gravel roads. They use a combination of inter-robot localization and direct follower-to-leader measurements. While operating only using maps created with simultaneous localization and mapping (SLAM) for localization, they observe that the performance degrades by about 5 cm RMSE compared with direct measurements of the leader.

This work investigates a specific application of convoying: cooperative cargo transport. The inter-robot distance requirements are much tighter for cooperative cargo transport than the general convoy case. Depending on how the cargo is constructed, there will be limits on the loads and kinematic degrees of freedom. For cargo operations, the interaction between the cargo and the robots is an important classifying feature. Using the taxonomy provided by Tuci et al. [16], our cargo transport is *grasped*, i.e., the cargo is kinematically fully-defined by the state of the convoy. For this reason, we omit related works in which robots interact by surrounding or pushing their cargo.

Breaking down existing approaches to grasped cargo transport, we identify two distinct types: those that allow inter-robot communication and those that do not. When looking to classify vehicular communication, Hussein et al. [17] note a large number of challenges for moving systems such as the fragmentation of the network, effect of high velocity on signals, and environmental effects of operating outdoors.

Systems that do not rely on communication eliminate this bottleneck and rely on reactive control schemes based on inter-robot measurements of distance or transferred force. In GEOMOVE, Rizzo et al. [18] develop a controller for large holonomic robots in a factory. The follower robot looks for lidar reflectors on the leader to estimate their relative pose. They demonstrate that the vehicles can maintain inter-robot separation errors of less than 5 cm. These robots use a common 2D lidar map for localization. Xie et al. [19] and Rauniyar et al. [20] use a combination of force sensing and lidar retro-reflector detections to carry a piece of cargo coupling two vehicles. The experiments are performed on a smooth indoor surface with holonomic vehicles at low speeds. Similarly, Huzaefa et al. [21] use force estimation to control UGVs. Their testing is also limited to an indoor

location with external state estimates, but they develop a method to control N UGVs that all connect directly to the common cargo.

Central control methods rely on communication to share either current state estimates from the robot or send final control commands to every vehicle. Stroupe et al. [22] demonstrate the ability to construct small structures using a pair of mobile robots with manipulators. While they are coupled through the cargo, force-torque sensing allows them to move cooperatively. Central communication is used to provide state estimates and commands for each vehicle. Zhang et al. [23] construct a pair of Ackermann robots and employ independent sliding-mode control on each vehicle to track a setpoint in front of the leader and the desired following position relative to that leader for the follower. Wireless communication between the two vehicles allows for the leader's position to be sent to the follower.

III. METHODS

Throughout this paper, we consider a robot convoy consisting of several Ackermann-steered vehicles. For the sake of conciseness, all methods are presented with a convoy of two robots, consisting of one leader and one follower as depicted in Fig. 1. We discuss the methods' capabilities to scale to multiple robots at the end of this section.

The current state of each robot, $\mathbf{T}(t) \in \text{SE}(2)$, is the pose at the center of the rear wheels with position $\mathbf{r}(t) = [x(t) \ y(t)]^T \in \mathbb{R}^2$ and orientation $\theta(t) \in \mathbb{R}$. The control inputs for each robot include its forward velocity and steering angle $\mathbf{u}(t) = [v(t) \ \delta(t)]^T \in \mathbb{R}^2$. It is assumed that the motion of each robot can be described using a standard kinematic non-slip bicycle model [24] with the ordinary differential equation (ODE),

$$f(\mathbf{T}(t), \mathbf{u}(t)) = \begin{bmatrix} \dot{x}(t) \\ \dot{y}(t) \\ \dot{\theta}(t) \end{bmatrix} = \begin{bmatrix} v(t) \cdot \sin(\theta(t)) \\ v(t) \cdot \cos(\theta(t)) \\ \frac{v(t)}{L} \cdot \tan(\delta(t)) \end{bmatrix}, \quad (1)$$

where L is the separation between front and rear wheels. The subscripts 'l' and 'f' will be used to denote which states and inputs correspond to the leader and follower respectively.

Our objective is to determine suitable control inputs for both robot systems, such that they accurately track a pre-defined reference path (in the following also called teach path) while simultaneously maintaining a desired inter-robot distance. The distance can be defined either in Euclidean space or along the arc length of the teach path. The former is applicable to the primary use case in which the robots are physically coupled to jointly transport cargo. In this setting, joints that constrain position but allow free rotation reduce the control problem to keeping the follower at the desired Euclidean distance from the leader.

A. System Overview

For implementation, we use a model-predictive control scheme with a prediction and control horizon of K robot states $\mathbf{T}_k = \mathbf{T}(t_k)$, where the sampling times t_k are spaced by ΔT . The MPC finds the optimal sequence of control

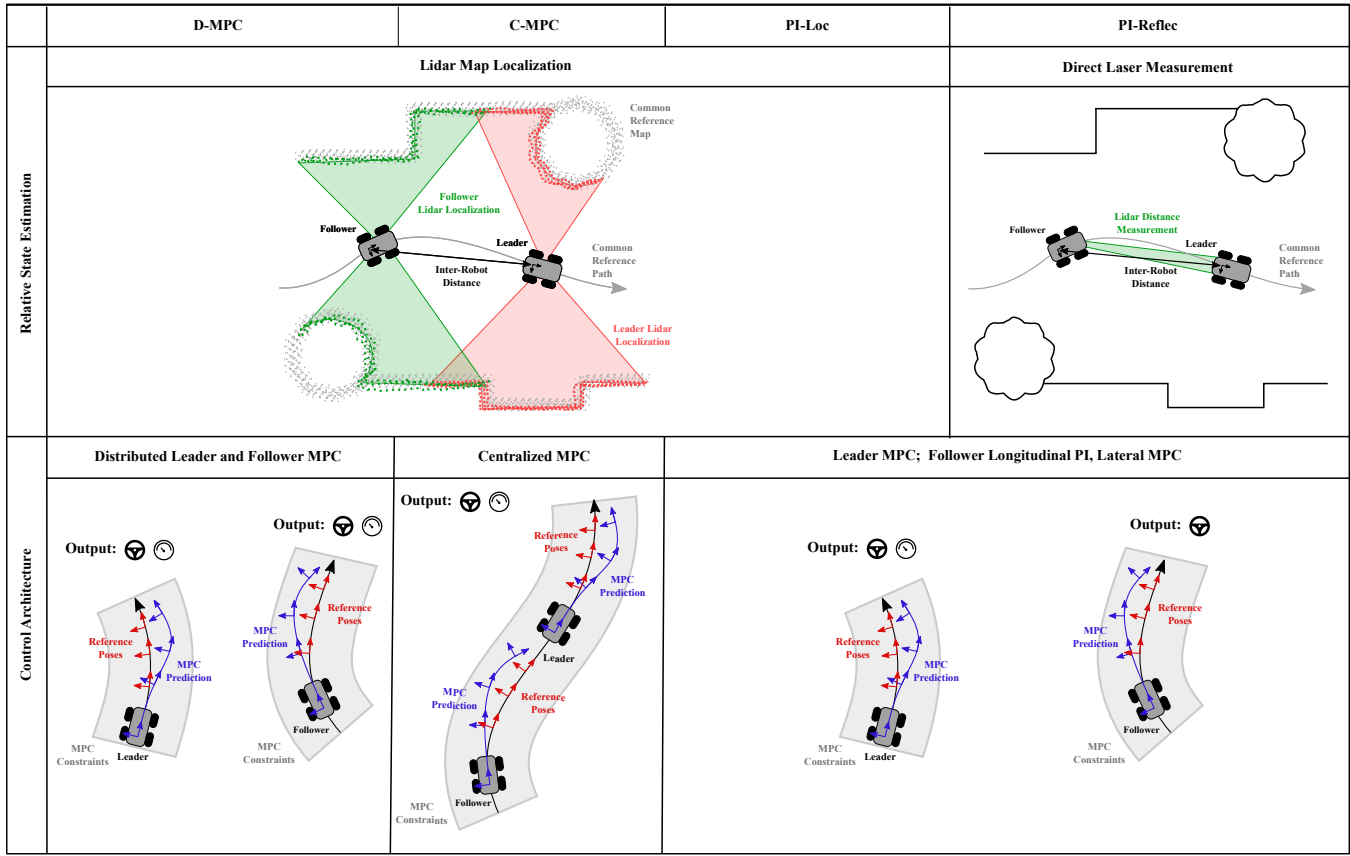


Fig. 2. The four controllers share similarities but are divided by how the inter-robot distance is measured and what variables are free for the MPC to optimize. All methods allow the steering angle to be controlled (steering wheel icon) but only some allow the linear velocity (gauge icon) to vary.

inputs $\mathbf{u}_k = \mathbf{u}(t_k)$ that minimize a cost function for path and inter-robot distance tracking, subject to constraints. This is guided by defining a set of suitable, discrete reference poses $\mathbf{T}_{\text{ref},k}$ for the robots along the teach path. A safe corridor, $\mathcal{X}_{\text{corr}}$, bounds the teach path, defining the maximum lateral error along the path. In this work, we focus on developing a distributed system in which each robot solves its own localization and control problems, requiring minimal communication between individual vehicles. Information flows only from the leader to the follower, enabling distribution across many robots. Additional MPC configurations are considered as baseline comparisons. Fig. 2 provides an overview of the different control architectures. The remainder of this section details the individual components of the proposed system.

B. Localization

Each robot runs the Visual Teach & Repeat (VT&R) navigation stack [8]. The localization is performed in $\text{SE}(3)$; however, we project onto $\text{SE}(2)$ for planning and control purposes. We assume that the teach phase has already been completed (using any one robot) and that each robot in the convoy maintains a local copy of the resulting teach path and submaps. Using this data, each robot is able to localize itself with respect to the teach path individually. While we use LiDAR localization for this work, the control approach is agnostic to the particular sensor modality. For details on teach path and submap construction and the localization

capabilities of VT&R, we refer readers to [25].

C. Reference Pose Planning

Using the successful localization of each robot, K discrete reference poses $\mathbf{T}_{\text{ref},k}$ at times t_k for both leader and follower are defined along the teach path in $\text{SE}(3)$.

1) *Leader Reference Poses*: The leader reference poses are defined using a desired forward velocity of the robot convoy. Given the desired convoy speed and the leader's current state (extrapolated from the most recent localization under a constant-velocity assumption), the reference poses can be defined along the teach path in a straightforward manner. We note that this reference pose selection is the baseline approach implemented in the latest version of VT&R [9].

2) *Follower Reference Poses*: For the follower reference pose planning, two alternative methods are considered. Both take the desired inter-robot distance explicitly into account.

a) *Distance-Aware Pose Selection*: The first method relies on an established communication link between leader and follower, defining reference poses for the follower that maintain the desired inter-robot distance using the latest information about the leader. The simplest approach uses the planned leader reference poses. For improved performance, the leader's state estimate and anticipated motion, obtained from its most recent MPC solution, can be used instead. A linear interpolation in the Lie algebra $\mathfrak{se}(3)$ of the MPC rollout provides the anticipated leader state at the follower's

reference times. Once the leader states at the desired times are determined, the follower reference poses are defined along the teach path such that they satisfy the inter-robot distance, either in Euclidean space or along the path's arc length. Because this method depends on the quality of the leader's state estimates and MPC tracking, errors can arise if these are inaccurate or biased. To address this, an alternative reference pose selection method is proposed that implements a proportional-integral (PI) feedback controller directly on the inter-robot distance error.

b) *PI Feedback Controller Pose Selection*: In the alternative method, a PI controller adjusts the follower's speed directly based on the current deviation from the desired inter-robot distance,

$$v_{\text{ref,f}}(t) = K_p e_{\text{dist}}(t) + K_i \int_0^t e_{\text{dist}}(\tau) d\tau, \quad (2)$$

where e_{dist} denotes the error from the desired inter-robot distance. The velocity obtained from this controller is assumed constant across the follower's reference poses, making the reference pose selection analogous to that of the leader. The main advantage of this approach is that it explicitly incorporates the inter-robot distance, allowing direct corrective action through proportional and integral feedback.

D. Model-Predictive Control Architectures

Three nonlinear MPC architectures are considered, each formulated in $\text{SE}(2)$ by projecting the robot's reference poses into the plane tangent to the nearest path segment. Two of those architectures are distributed, while an additional centralized method is investigated for comparison. Each architecture considers a common set of cost terms and constraints. The cost terms are given as

$$J_{\text{ref},k} = \ln(\mathbf{T}_{\text{ref},k} \mathbf{T}_k^{-1})^{\vee T} \mathbf{Q}_{\text{ref}}^{-1} \ln(\mathbf{T}_{\text{ref},k} \mathbf{T}_k^{-1})^{\vee}, \quad (3a)$$

$$J_{\text{cont},k} = \mathbf{u}_k^T \mathbf{Q}_{\text{cont}}^{-1} \mathbf{u}_k, \quad (3b)$$

$$J_{\text{acc},k} = (\mathbf{u}_k - \mathbf{u}_{k-1})^T \mathbf{Q}_{\text{acc}}^{-1} (\mathbf{u}_k - \mathbf{u}_{k-1}), \quad (3c)$$

$$J_{\text{dist},k} = \|\mathbf{r}_{\text{l},k} - \mathbf{r}_{\text{f},k}\|_2^T \mathbf{Q}_{\text{dist}}^{-1} \|\mathbf{r}_{\text{l},k} - \mathbf{r}_{\text{f},k}\|_2, \quad (3d)$$

where J_{ref} controls reference pose tracking, J_{cont} reduces control input magnitude, J_{acc} reduces acceleration, and J_{dist} controls the inter-robot distance. $\ln(\mathbf{T})^{\vee}$ transforms an element $\mathbf{T} \in \text{SE}(2)$ into the 3×1 element of the Lie algebra $\mathfrak{se}(2)$. The weighting matrices \mathbf{Q} for each cost term are constant.

The constraints are given as

$$g_{\text{model},k} : \mathbf{T}_k - \int_{t_{k-1}}^{t_k} f(\mathbf{T}(t), \mathbf{u}(t)) dt = 0, \quad (4a)$$

$$g_{\text{cont},k} : \mathbf{u}_{\text{min}} < \mathbf{u}_k < \mathbf{u}_{\text{max}}, \quad (4b)$$

$$g_{\text{acc},k} : \Delta \mathbf{u}_{\text{min}} < \mathbf{u}_k - \mathbf{u}_{k-1} < \Delta \mathbf{u}_{\text{max}}, \quad (4c)$$

$$g_{\text{corr},k} : \mathbf{r}_k \in \mathcal{X}_{\text{corr}}, \quad (4d)$$

$$g_{\text{dist},k} : d_{\text{min}} < \|\mathbf{r}_{\text{l},k} - \mathbf{r}_{\text{f},k}\|_2 < d_{\text{max}}, \quad (4e)$$

where g_{model} enforces adherence to the kinematic motion model, g_{cont} limits the control input magnitude, and g_{acc} limits acceleration. Additionally, g_{corr} ensures that the robots

remain within the safe corridor $\mathcal{X}_{\text{corr}}$ around the path and g_{dist} maintains a collision-free inter-robot distance, given minimum and maximum distances d_{min} and d_{max} . During implementation, (4a) is solved numerically, using a Runge-Kutta (4,5) method, assuming constant control inputs over interval $[t_{k-1}, t_k]$ and accounting for a first-order lag.

Next, we discuss how these cost terms and constraints are assembled into optimization problems for each controller. The resulting problems are implemented using CasADi [26].

1) *Distributed MPC*: We propose a distributed MPC architecture, which solves for the control inputs of the leader and follower individually. This means that each robot solves their respective control optimization problem locally. The optimization problem for the leader can be written as

$$\begin{aligned} \operatorname{argmin}_{\mathbf{T}_{\text{l},k}, \mathbf{u}_{\text{l},k}} \quad & \sum_{k=1}^K J_{\text{ref},\text{l},k} + J_{\text{cont},\text{l},k} + J_{\text{acc},\text{l},k} \\ \text{s.t.} \quad & \forall k \in 1, 2, \dots, K \\ & g_{\text{model},\text{l},k}, g_{\text{cont},\text{l},k}, g_{\text{acc},\text{l},k}, g_{\text{corr},\text{l},k} \end{aligned} \quad (5)$$

which optimizes for the leader's states, $\mathbf{T}_{\text{l},k}$, and inputs, $\mathbf{u}_{\text{l},k}$, at each discrete time t_k during the prediction horizon. The objective function includes the reference pose tracking as well as control input magnitude, and acceleration for the leader. The motion model, control input magnitude, acceleration, and corridor constraints are active.

Analogously, the optimization problem for the follower can be written as

$$\begin{aligned} \operatorname{argmin}_{\mathbf{T}_{\text{f},k}, \mathbf{u}_{\text{f},k}} \quad & \sum_{k=1}^K J_{\text{ref},\text{f},k} + J_{\text{cont},\text{f},k} + J_{\text{acc},\text{f},k} + J_{\text{dist},k} \\ \text{s.t.} \quad & \forall k \in 1, 2, \dots, K \\ & g_{\text{model},\text{f},k}, g_{\text{cont},\text{f},k}, g_{\text{acc},\text{f},k}, g_{\text{corr},\text{f},k}, g_{\text{dist},k} \end{aligned} \quad (6)$$

The objective function includes the additional cost term and constraint for the inter-robot distance. The key innovation in this paper is passing the MPC solution from the leader back to the follower. Interpolating the real solution has better performance than the reference poses or the current state alone. The computation of these terms as well as the definition of the reference poses utilize the last reported localization result and MPC prediction from the leader. This method requires an established communication link. In the discussion, this method is abbreviated D-MPC.

2) *Centralized MPC*: As a non-scalable baseline to the proposed distributed MPC architecture, a centralized implementation is also considered. Here, the states and control inputs to both robots are solved in one optimization problem, formulated as

$$\begin{aligned} \operatorname{argmin}_{\mathbf{T}_{\text{l},k}, \mathbf{u}_{\text{l},k}, \mathbf{T}_{\text{f},k}, \mathbf{u}_{\text{f},k}} \quad & \sum_{k=1}^K J_{\text{ref},\text{l},k} + J_{\text{cont},\text{l},k} + J_{\text{acc},\text{l},k} \\ & + J_{\text{ref},\text{f},k} + J_{\text{cont},\text{f},k} + J_{\text{acc},\text{f},k} + J_{\text{dist},k} \\ \text{s.t.} \quad & \forall k \in 1, 2, \dots, K \\ & g_{\text{model},\text{l},k}, g_{\text{cont},\text{l},k}, g_{\text{acc},\text{l},k}, g_{\text{corr},\text{l},k}, \\ & g_{\text{model},\text{f},k}, g_{\text{cont},\text{f},k}, g_{\text{acc},\text{f},k}, g_{\text{corr},\text{f},k}, g_{\text{dist},k} \end{aligned} \quad (7)$$

This problem includes all optimization variables, cost terms and constraints from the two distributed ones. The distance cost term and constraints are adapted to use the distance between the variable leader and follower poses. Additionally, the follower's reference poses are defined with respect to the leader's reference poses, because the leader's MPC has not yet been solved. The solution can be computed on either the leader or follower and requires an established communication link. In the discussion, this method is abbreviated as C-MPC.

3) *Independent Lateral and Longitudinal Control*: Lastly, we consider a control architecture that utilizes the reference pose selection based on the PI feedback controller. This architecture is distributed, and the optimization problem for the leader remains (5). The reference poses for the follower are defined according to the velocity computed by the PI controller on the inter-robot distance. Additionally, this velocity is added as an equality constraint and the optimization problem for the follower MPC becomes

$$\begin{aligned} \operatorname{argmin}_{\mathbf{T}_{f,k}, \mathbf{u}_{f,k}} \quad & \sum_{k=1}^K J_{\text{ref},f,k} + J_{\text{cont},f,k} + J_{\text{acc},f,k} \\ \text{s.t.} \quad & \forall k \in 1, 2, \dots, K \end{aligned} \quad (8)$$

$$g_{\text{model},f,k}, g_{\text{cont},f,k}, g_{\text{acc},f,k}, g_{\text{corr},f,k}, v_{f,k} = v_{\text{ref},f}$$

Due to the linear velocity constraint, the MPC can select only the steering angles. This decouples the lateral and longitudinal control of the robot, with the former being selected by the MPC and the latter by the PI controller.

We evaluate two cases for this controller. In the first, the inter-robot distance is computed from the most recent localization results of the leader and follower, requiring a communication link. In the discussion, this is abbreviated PI-Loc. In the second, the distance is measured directly, e.g., via line of sight, eliminating the need for communication. In the discussion, this is abbreviated PI-Reflec.

E. Scaling to N Robots

The primary advantage of distributed control approaches is scalability. Adding another follower to the convoy is straightforward, as information flows only from the leader to the follower. Technically, each follower can consider any existing robot in the convoy as their leader. In practice, the most stable configuration uses one common leader for every follower, so disturbances in one follower's motion will not propagate through the chain of robots. However, depending on the convoy length and chosen approach, communication links or distance measurements could make a chained following pattern more desirable.

The C-MPC approach is difficult to scale. Adding more coupled variables to the optimization problem increases complexity and solve time. While this effect is insignificant for two robots, quadratic scaling is expected from the utilized *ipopt* solver [27]. This may limit the effectiveness for large convoys. Additional practical challenges include the required *a priori* knowledge of the robot kinematics of every vehicle in the convoy and the software engineering needed to scale to an arbitrary number of followers.

TABLE I
EVALUATION ROUTE SUMMARIES

Name	Length	# Trials	Total Distance	Terrain
Tennis	113 m	12	1.7 km	Cracked but smooth cement.
Parking	200 m	12	2.4 km	Asphalt parking lot.
Dome	260 m	15	3.9 km	Mowed grass lawn.
Hillside	180 m	12	2.51 km	Mowed grass. $\pm 10^\circ$ roll and pitch inclines.
Woody	278 m	4	1.11 km	Tall grass, branches, potholes.

IV. EXPERIMENTAL SETUP

For the quantitative experiments, we use a pair of AgileX Hunter 2.0 vehicles. These robots have Ackermann steering and rear-wheel drive. An Ouster OS-0 128 beam lidar is mounted on top of each vehicle and is used for localization and mapping. A mock cargo connects the robots, e.f. Fig 1. Kinematically, the cargo has a prismatic joint along its length with a travel range of ± 27 cm. A loose pin joint on each vehicle connects it to the cargo. The loose pins act as spherical joints; although, the flatness of the cargo means that roll is minimized but not constrained. Routers on each robot connect to each other and messages are passed using the ROS2 Zenoh [28] middleware. A retro-reflective panel is placed on the back of the leader. Segmenting these points and using a robust plane-fit provides the direct measurement of the leader's distance from the follower. This signal is used to evaluate the quality of all controllers. This measurement was validated by a high-framerate video of a tape measure as it extends while the vehicles were in motion.

Four loops are evaluated three times for each controller. The convoy has nominal forward speed of 0.7 m/s. The terrain has a significant impact on the quality of single-robot navigation so we choose paths that are progressively more difficult for the system to handle. In the Woody loop, the follower sometimes loses track of the leader. As this is our evaluation signal, the Woody Loop was used only for qualitative analysis. A summary of the paths is provided in Table I. The supplementary video provides samples of the convoy operating in all environments.

V. QUANTITATIVE RESULTS

The results in Table II quantify high-level patterns that were anticipated. The Centralized and Distributed MPCs have no integral-type term and exhibit a bias on all loops tested. The PI controllers have almost no bias in steady-state, regardless of how the control signal is estimated, because the integral term drives the average error to zero. When the terrain is smooth and the robots' reactions match the MPC predictions, the error variance and maxima are similar between the MPC controllers and the direct measurement of the leader. Only on the Hillside Loop does the direct measurement of the leader appear to lead to meaningfully smaller standard deviation of 4.2 cm vs 5.6 cm for the distributed MPC. Investigating the locations along the path where the largest errors occur, we observe that tight corners

TABLE II

ERROR METRICS FOR FOUR CONVOYED ROUTES. EACH COLUMN REPRESENTS THE RESULTS FROM THREE EXPERIMENTS ON THE ROUTE.
ALL VALUES ARE IN CM.

Relative State Est.	Lidar Map Localization			Laser Meas.	
Controller	D-MPC (Ours)	C-MPC	PI-Loc	PI-Reflec	
Parking Lot Loop					
Euclidean Distance	Mean Err.	-2.1	-4.7	0.7	0.4
	RMSE	3.9	6.0	6.9	3.2
	Std. Dev.	3.2	3.7	6.9	3.2
	Max Err.	12.9	18.7	27.6	19.4
Path Tracking	Lead. RMSE	2.9	2.7	2.7	2.7
	Lead. Max Err.	7.4	7.4	7.2	7.1
	Fol. RMSE	5.3	5.3	5.3	5.2
	Fol. Max Err.	10.2	10.7	8.7	10.3
Mars Dome Loop					
Euclidean Distance	Mean Err.	-2.6	-2.6	1.8	0.3
	RMSE	5.0	4.9	6.1	5.0
	Std. Dev.	4.3	4.1	5.8	3.4
	Max Err.	-17.3	-16.5	26.6	18.8
Path Tracking	Lead. RMSE	2.8	2.7	2.9	2.9
	Lead. Max Err.	9.8	9.2	10.7	10.5
	Fol. RMSE	4.5	4.6	4.4	4.4
	Fol. Max Err.	10.3	10.3	10.0	9.8
Tennis Court Loop					
Euclidean Distance	Mean Err.	-2.2	-2.2	1.3	0.5
	RMSE	4.3	4.5	6.1	3.7
	Std. Dev.	3.7	3.9	5.9	3.7
	Max Err.	-14.8	-15.1	26.7	19.1
Path Tracking	Lead. RMSE	5.1	4.8	5.4	5.6
	Lead. Max Err.	13.7	11.4	14.6	15.4
	Fol. RMSE	5.4	5.6	5.1	4.9
	Fol. Max Err.	13.2	14.7	13.1	11.2
Hilside Loop					
Euclidean Distance	Mean Err.	-3.5	-3.3	0.7	0.3
	RMSE	6.6	6.6	7.5	4.2
	Std. Dev.	5.6	5.8	7.5	4.2
	Max Err.	19.5	-29.8	-27.8	18.2
Path Tracking	Lead. RMSE	7.2	6.7	6.9	7.1
	Lead. Max Err.	28.1	26.2	22.7	26.7
	Fol. RMSE	6.1	6.4	5.9	6.1
	Fol. Max Err.	22.4	20.5	21.2	18.7

and changes in slope lead to errors for the MPCs. Tight corners challenge all controllers, as the response of the vehicle becomes less ideal close to its mechanical limits. More interestingly, the 2D projection of the target path for the MPC leads to a discrepancy between the predicted location of the leader and the true path. This is most visible when the leader is about to crest a hill. The MPC prediction will continue to climb in the local plane of the leader, even though during that rollout, the slope ends and the robot will return to a flatter orientation. The follower selects target positions to maintain the Euclidean distance to the leader's rollout but executing these commands leads to the robots becoming too close together as the follower thinks the leader will fly above the terrain. In the future, considering the local shape of the path along the rollout might help to mitigate this issue.

The two MPCs cause a consistent separation bias of approximately 3 cm too close. To investigate the cause of this bias, the D-MPC test on the Mars Dome Loop was duplicated with the convoying order of the robots switched. The results of this investigation are presented in Table III. We find that the bias has the opposite sign in this configuration. In the default configuration, with Robot A as the leader, the bias is -2.7 cm; however, when Robot A is the follower the bias is +2.2 cm. This points to a hardware-specific bias from one or both robots. Practically, these biases are constant enough throughout the different testing environments that a constant offset could be applied to correct it for a fixed pair of vehicles.

In Table III, the RMS path-tracking error of Robot A is 2.8 cm and 2.9 cm as leader and follower, respectively. Similarly, Robot B has RMS errors of 4.4 cm and 4.5 cm as leader and follower. This suggests that the individual tuning of the single-robot path tracking is the primary effect rather than the

role of leader or follower. This makes sense, as the reference path of the follower is always on the taught path regardless of the leader's position. This shows that the following methods do not reduce the quality of path tracking while in a convoy.

The MPCs perform better while the leader accelerates than the PI controllers. For example, when the convoy starts to move, the future knowledge of the leader's state allows the follower to match the acceleration profile and maintain the target better than the reactive controllers. Fig. 3 shows the inter-robot separation over the first 4 m of forward travel on the flat Tennis Court Loop. D-MPC maintains the target most accurately during acceleration while the reactive controllers causes the follower to lag behind for approximately 3 m of transient behaviours.

VI. QUALITATIVE RESULTS

A primary advantage of using a distributed MPC instead of a centralized one is the flexibility with respect to the composition of the multi-robot system. For a centralized MPC, the order and kinematic model must be known ahead of time, whereas in the distributed case, robots may be added or removed from the convoy easily. We demonstrate this flexibility by adding a smaller Hunter SE to the front of

TABLE III
THE EFFECT OF ROBOT ORDER ON PERFORMANCE. TESTED ON THE MARS DOME LOOP USING THE D-MPC. ALL VALUES ARE IN CM.

	Robot A leads	Robot B leads
Euclidean Distance	Mean Error	-2.7
	RMSE	5.1
	Standard Deviation	4.3
	Max Error	-17.3
Path Tracking	Leader RMSE	2.8
	Leader Max Error	9.8
	Follower RMSE	4.5
	Follower Max Error	10.3

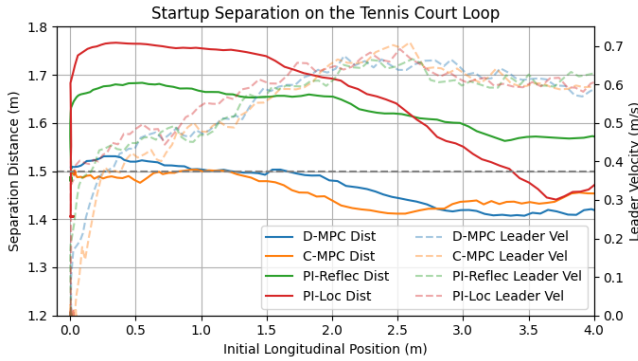


Fig. 3. Startup separation as the robots start to move. The MPC controllers maintain close to the target of 1.5 m from the initial motion. The lighter colours show the velocity of the leader as it accelerates from rest.

convoy as shown in Fig. 4. The only reconfiguration of note was the networking to allow the sharing of MPC rollouts to the new vehicle. In our formulation of the distributed MPC, subsequent followers can subscribe to the rollout of the preceding robot or the leader at the front of the convoy. In our testing, following a common leader is advantageous as transient disturbances to one follower do not propagate down the chain. Another advantage of the distributed approach is that the vehicles in the convoy do not require knowledge of each other. If every robot publishes its MPC trajectory and follows a leader's trajectory, the details of the robot's kinematics or controller are irrelevant.

The Euclidean-distance reference-pose planning method can be easily replaced with one using the path length between the robots. This represents a more common large-convoy setup where each robot is a common arc-length distance from each other [14]. The supplementary video shows a comparison around sharp corners of the Euclidean-distance and arc-length modes. Sharp turns lead to the most significant behavioural change. A path-length implementation is difficult with a direct measurement of the leader's position.

The quality of tracking is sensitive to the network delay. Longer delays require interpolation further along the leader's MPC predictions which are less accurate. An et al. [29] investigate some common network architectures used for collaborative cargo transport and in future work we aim to further benchmark the effect of the network stability, especially as a new robot joins the convoy.

The D-MPC and PI-Reflec controllers perform more reliably than C-MPC and PI-Loc. Additionally, due to their distributed nature, both are scalable to longer convoy chains. On rapid elevation changes, using a direct measurement of the leader's relative position could be advantageous. However, the D-MPC approach provides more flexibility as the robots can convoy beyond line of sight and longer convoys are unaffected by disturbances along the chain. The D-MPC makes the fewest assumptions about the operating environment and geometric arrangement of the convoy, which makes it widely applicable.



Fig. 4. A three-robot convoy repeating in unison using the Distributed MPC approach presented here. Extending the system to N robots is simple with the distributed MPC.

VII. CONCLUSION

A distributed model-predictive controller for cooperative cargo transport was developed and tested on over 3 km of convoyed driving. The Euclidean distance between the cargo mounting pins is controlled to ensure that even as the robots go around curves, the cargo remains the correct distance between each vehicle. The inter-robot separation depends on the quality of path tracking by each Ackermann robot. On paved surfaces, the convoy achieves inter-robot separation RMSE of 3.9 cm and path-tracking RMSE of 5.3 cm. As the terrain roughness and slope increase, the performance degrades to 6.6 cm RMSE. Finally, we demonstrated additional use cases that are available with only configuration changes to the distributed MPC. When robots do not require Euclidean separation, the reference poses can be selected to maintain an arc-length separation. Additional following robots can be easily added to the convoy with either the Euclidean or arc-length distances to any other vehicle in the system. This flexibility supports the original motivation of collaborative cargo transport, allowing a group of robots to work together when required and easily separated when not.

ACKNOWLEDGMENT

A.K. holds a Vanier Canada Graduate Scholarship.

REFERENCES

- [1] I. Ermolov, “Industrial Robotics Review,” in *Robotics: Industry 4.0 Issues & New Intelligent Control Paradigms*, A. G. Kravets, Ed., Cham: Springer International Publishing, 2020, pp. 195–204.
- [2] P. Slowik and B. Sharpe, *Automation in the long haul: Challenges and opportunities of autonomous heavy-duty trucking in the United States*, Mar. 2018.
- [3] P. F. Lima, M. Nilsson, M. Trincavelli, J. Mårtensson, and B. Wahlberg, “Spatial Model Predictive Control for Smooth and Accurate Steering of an Autonomous Truck,” *IEEE Trans. Intell. Veh.*, vol. 2, no. 4, pp. 238–250, Dec. 2017.
- [4] K. S. Saidi, T. Bock, and C. Georgoulas, “Robotics in Construction,” in *Springer Handbook of Robotics*, B. Siciliano and O. Khatib, Eds., Cham: Springer International Publishing, 2016, pp. 1493–1520.

[5] J. A. Marshall, A. Bonchis, E. Nebot, and S. Scheding, "Robotics in Mining," in *Springer Handbook of Robotics*, B. Siciliano and O. Khatib, Eds., Cham: Springer International Publishing, 2016, pp. 1549–1576.

[6] J. Marshall, T. Barfoot, and J. Larsson, "Autonomous underground tramsing for center-articulated vehicles," *J. Field Robot.*, vol. 25, no. 6-7, pp. 400–421, 2008.

[7] B. Tian, J. Yang, C. Zhang, X. Hao, S. Meng, S. Wang, Z. Yang, L. Chen, Y. Zhao, and S. Ge, "Autonomous Driving in Underground Mines via Parallel Driving Operation Systems: Challenges, Frameworks and Cases Study," *IEEE Trans. Intell. Veh.*, vol. 10, no. 5, pp. 3268–3277, May 2025.

[8] P. Furgale and T. D. Barfoot, "Visual teach and repeat for long-range rover autonomy," *J. Field Robot.*, vol. 27, no. 5, pp. 534–560, 2010.

[9] X. Qiao, A. Krawciw, S. Lilge, and T. D. Barfoot, "Radar Teach and Repeat: Architecture and Initial Field Testing," in *2025 IEEE Int. Conf. Robot. Autom. ICRA*, May 2025, pp. 13 021–13 027.

[10] K. Burnett, Y. Wu, D. J. Yoon, A. P. Schoellig, and T. D. Barfoot, "Are We Ready for Radar to Replace Lidar in All-Weather Mapping and Localization?" *IEEE Robot. Autom. Lett.*, vol. 7, no. 4, pp. 10 328–10 335, Oct. 2022.

[11] S. Nahavandi, S. Mohamed, I. Hossain, D. Nahavandi, S. M. Salaken, M. Rokonuzzaman, R. Ayoub, and R. Smith, "Autonomous Convoying: A Survey on Current Research and Development," *IEEE Access*, vol. 10, pp. 13 663–13 683, 2022.

[12] V. Lesch, M. Breitbach, M. Segata, C. Becker, S. Kounev, and C. Krupitzer, "An Overview on Approaches for Coordination of Platoons," *IEEE Trans. Intell. Trans. Sys.*, vol. 23, no. 8, pp. 10 049–10 065, Aug. 2022.

[13] X. Zhao, W. Yao, N. Li, and Y. Wang, "Design of leader's path following system for multi-vehicle autonomous convoy," in *2017 IEEE Int. Conf. Unmanned Syst. ICUS*, Oct. 2017, pp. 132–138.

[14] L. Vasseur, O. Lecointe, J. Dento, N. Cherfaoui, V. Marion, and J. G. Morillon, "Leader-follower function for autonomous military convoys," in *Unmanned Ground Veh. Technol. VI*, vol. 5422, SPIE, Sep. 2004, pp. 326–337.

[15] A. Bienemann, L. Beer, A. Reich, T. Steinecker, B. Forkel, A. Backhaus, P. Berthold, J. D. González, P. Mortimer, T. Luettel, and M. Maehlisch, "A Perception-Based Architecture for Autonomous Convoying in GNSS-Denied Areas," *IEEE Trans. Field Robot.*, pp. 1–1, 2025.

[16] E. Tuci, M. H. M. Alkilabi, and O. Akanyeti, "Cooperative Object Transport in Multi-Robot Systems: A Review of the State-of-the-Art," *Front. Robot. AI*, vol. 5, May 2018.

[17] N. H. Hussein, C. T. Yaw, S. P. Koh, S. K. Tiong, and K. H. Chong, "A Comprehensive Survey on Vehicular Networking: Communications, Applications, Challenges, and Upcoming Research Directions," *IEEE Access*, vol. 10, pp. 86 127–86 180, 2022.

[18] C. Rizzo, A. Lagraña, and D. Serrano, "GEOMOVE: Detached AGVs for Cooperative Transportation of Large and Heavy Loads in the Aeronautic Industry," in *2020 IEEE Int. Conf. Auton. Robot Syst. Compet. ICARSC*, Apr. 2020, pp. 126–133.

[19] F. Xie, H. Liu, M. Li, and M. Xia, "A LiDAR-Based Dual-Vehicle Collaborative Transportation Approach Without Communication," *IEEE Access*, vol. 13, pp. 104 406–104 421, 2025.

[20] A. Rauniyar, H. C. Upreti, A. Mishra, and P. Sethuramalingam, "MeWBots: Mecanum-Wheeled Robots for Collaborative Manipulation in an Obstacle-Clustered Environment Without Communication," *J. Intell. Robot Syst.*, vol. 102, no. 1, p. 3, May 2021.

[21] F. Huzaefa and Y.-C. Liu, "Force Distribution and Estimation for Cooperative Transportation Control on Multiple Unmanned Ground Vehicles," *IEEE Trans. Cybern.*, vol. 53, no. 2, pp. 1335–1347, Feb. 2023.

[22] A. Stroupe, T. Huntsberger, A. Okon, H. Aghazarian, and M. Robinson, "Behavior-based multi-robot collaboration for autonomous construction tasks," in *2005 IEEE/RSJ Int. Conf. Intell. Robots Syst.*, Aug. 2005, pp. 1495–1500.

[23] Q. Zhang, W. Li, L. Guo, and X. Qi, "Collaborative Transport Strategy for Dual AGVs in Smart Ports: Enhancing Docking Accuracy in No-Load Formations," *J. of Marine Sci. and Eng.*, vol. 13, no. 1, p. 81, Jan. 2025.

[24] J. Kong, M. Pfeiffer, G. Schildbach, and F. Borrelli, "Kinematic and dynamic vehicle models for autonomous driving control design," in *2015 IEEE Intell. Veh. Symp.*, Jun. 2015, pp. 1094–1099.

[25] Y. Wu, "VT&R3: Generalizing the Teach and Repeat Navigation Framework," MSc, University of Toronto, Toronto, Canada, Sep. 2022.

[26] J. A. E. Andersson, J. Gillis, G. Horn, J. B. Rawlings, and M. Diehl, "CasADi – A software framework for nonlinear optimization and optimal control," *Math. Program. Comput.*, vol. 11, no. 1, pp. 1–36, 2019.

[27] A. Wächter and L. T. Biegler, "On the implementation of an interior-point filter line-search algorithm for large-scale nonlinear programming," *Math. Program.*, vol. 106, no. 1, pp. 25–57, Mar. 2006.

[28] Zenoh, Eclipse Foundation. <https://zenoh.io/>.

[29] X. An, C. Wu, Y. Lin, M. Lin, T. Yoshinaga, and Y. Ji, "Multi-Robot Systems and Cooperative Object Transport: Communications, Platforms, and Challenges," *IEEE Open J. Comput. Soc.*, vol. 4, pp. 23–36, 2023.